

# High accuracy transfer printing of III-V/SOI micro-disk resonators for non-linear applications

John McPhillimy<sup>1</sup>, Charalambos Klitis<sup>2</sup>, Stuart May<sup>2</sup>, Benoit Guilhabert<sup>1</sup>, Martin D. Dawson<sup>1</sup>, Marc Sorel<sup>2</sup>, and Michael J. Strain<sup>1</sup>

<sup>1</sup> Institute of Photonics, Dept. of Physics, University of Strathclyde, Glasgow G1 1RD, UK

<sup>2</sup> School of Engineering, University of Glasgow, Glasgow, G12 8LT, UK

*e-mail: john.mcphillimy@strath.ac.uk*

## ABSTRACT

In this paper, we report on the heterogeneous integration of III-V-on-silicon micro-disk resonators using our high alignment accuracy transfer printing method, exhibiting loaded quality factors of  $\approx 2.5 \times 10^4$ . High absolute positional printing accuracy allows control over the devices lateral coupling gap to the silicon bus waveguide, enabling selective resonant mode excitation within the multimode micro-disk. We further report efficient non-linear conversion by four-wave mixing. A conversion efficiency of -25dB is obtained at an on-chip optical power of 2.5mW.

**Keywords:** Photonic Integrated Circuits, Hybrid integration, Transfer Printing, Silicon photonics, III-V semiconductors, Nonlinear optics

## 1. INTRODUCTION

Silicon-on-insulator (SOI) has become the standard material for the realisation of large-scale photonic integrated circuits (PICs). Its compatibility with silicon's CMOS manufacturing and high index contrast allow extremely compact device footprints, whilst its wide transparency window at the telecom wavelengths makes it suitable for a large range of applications [1]. However, limitations such as its inefficient light generation at the telecom wavelengths to its lack of a  $\chi^{(2)}$  non-linearity inhibit the production of a full suite of photonic components necessary for highly functional PIC technology. In relation to this, the heterogeneous integration of multiple device platforms is becoming the primary method for producing integrated photonic systems which can enable future applications in areas such as telecommunications, optical sensing technologies and quantum systems [2, 3].

One area greatly benefited by integrated photonics is non-linear optics. The highly compact device geometries of on-chip integrated systems, compared to the fibre-scale architectures, enables much higher modal confinements for increased light-matter interactions over shorter distances. Many different planar material platforms are being investigated, including aluminium gallium arsenide (AlGaAs) and silicon, with the optimum platform exhibiting strong non-linear properties yet providing high-yield processing capabilities [4]. Silicon has a high  $\chi^{(3)}$  material non-linearity however it suffers from two-photon absorption (TPA) when operated at the telecom wavelengths, limiting the possible non-linear applications [5]. Alternatively, AlGaAs is another promising candidate with its large refractive index ( $n=3.3$ ), large transparency window and high  $\chi^{(3)}$  non-linearity [6]. Further to this, the ability to engineer its bandgap means that its TPA can be mitigated benefiting non-linear processes such as four-wave mixing (FWM) [7].

We propose the direct integration of fully fabricated AlGaAs resonators with pre-processed silicon waveguides on the SOI platform, combining both the highly non-linear properties of AlGaAs alongside the manufacturing capabilities of silicon. One potential approach to achieve this is by using transfer printing (TP). TP follows the detachment of a pre-processed device from its native substrate which is then transferred and bonded onto a receiver platform [8]. It also allows the dense integration of hybrid devices over multiple platforms all onto a single-chip making it suitable for the production of large-scale PICs. TP has already been established as a means for producing hybrid devices, with demonstrations ranging from III-V-Si on-chip lasers [9] to micro-LED arrays [10]. Using our high alignment TP technique enables the back-end micro-assembly of efficient passive platforms, where we have recently shown the vertical integration of silicon passive devices as well as the hybrid assembly of silicon and III-V resonators [11,12].

In this work, AlGaAs micro-disk resonators of varying diameters are fully fabricated on their native substrate before being transfer printed on to Si bus waveguides to produce high quality factor hybrid resonator devices. The high alignment accuracy allows selective mode excitation within the disk resonators by control over the lateral coupling gap of the disk resonator and Si waveguide. We further report the non-linear optical characterisation of the hybrid resonators by achieving efficient FWM at low optical on-chip powers. Fabrication and micro-assembly techniques will be detailed along with accompanying experimental results.

## 2. FABRICATION OF III-V DISK RESONATORS

III-V micro-disk resonators are fabricated from an AlGaAs epitaxially grown material stack on top of a GaAs substrate. Control over the aluminium content of the  $\text{Al}_x\text{Ga}_{1-x}\text{As}$  enables the production of highly selective sacrificial layers which can be used to isolate AlGaAs structures from the GaAs substrate. For this work an  $\text{Al}_{0.3}\text{Ga}_{0.7}\text{As}$  layer of 270 nm thickness is grown on a high aluminium content  $\text{Al}_{0.9}\text{Ga}_{0.1}\text{As}$  sacrificial layer of 0.5  $\mu\text{m}$ , Fig. 1(a). Micro-disk structures, of diameters ranging from 3  $\mu\text{m}$  to 20  $\mu\text{m}$ , are patterned using electron-beam lithography into a deposited HSQ resist (Fig. 1(b)) with the pattern fully etched through to the GaAs substrate using reactive ion etching, Fig. 1(c). Unlike previous transfer printing work, no support anchors are used due to the whispering gallery modes being guided in close proximity to the disk sidewalls. Following this, a buffered HF acid selectively etches the high aluminium content  $\text{Al}_{0.9}\text{Ga}_{0.1}\text{As}$ , which when fully removed, will release the  $\text{Al}_{0.3}\text{Ga}_{0.7}\text{As}$  structures onto the GaAs substrate ready for transfer printing.

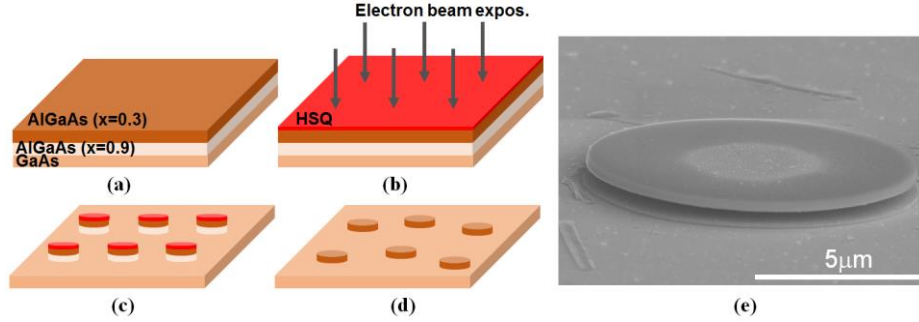


Fig 1. Schematic illustration of fabrication procedure showing (a) AlGaAs-On-GaAs substrate; (b) HSQ resist deposition and structure patterning through e-beam lithography; (c) RIE etch through to GaAs substrate leaving patterned structures of the AlGaAs stack; (d) Wet etch of sacrificial layer leaving AlGaAs disk structures distributed on the GaAs substrate, ready for transfer printing procedure; (e) SEM image of micro-disk structure on GaAs substrate with partially etched sacrificial layer.

## 3. TRANSFER PRINTED III-V-SOI DISK RESONATORS

The SOI receiver is comprised of a 220nm Si layer above a 2  $\mu\text{m}$  buried oxide. Ultra-thin Si waveguides of 220nm $\times$ 500nm for single-mode TE propagation are patterned by e-beam lithography before fabricated into the Si by RIE etch processes, with a 100nm thick HSQ upper cladding deposited producing a planar top surface. The TP procedure detaches the disk structure from its native substrate and transfers it to the receiving substrate using a polydimethylsiloxane (PDMS) stamp, made possible by the reversible adhesion properties of the PDMS as shown in Fig. 2(a). The PDMS stamp is brought into contact with the micro-disk structure, with a quick retraction of the stamp overcoming the bond strength and releasing the micro-disk from its native substrate. Once it is moved to its pre-defined position on the receiver substrate, the device is contacted with the surface before a slow retraction of the stamp releases the device, where it is bonded to the substrate. The printing procedure uses no intermediate adhesion layers, relying on the Van der Waal bonding between the micro-disk and substrate below. For alignment, the absolute position of the disk structure is calculated using optical microscopy techniques in relation to the receiving substrate's registration markers. This produces an absolute placement accuracy of  $\approx 100\text{nm}$  [12].

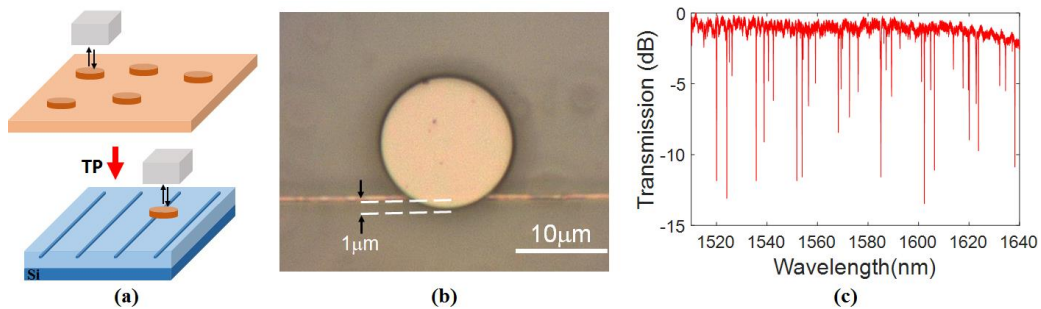


Fig 2. (a) Schematic illustration of transfer printing procedure of micro-disk structure from native substrate to SOI receiver bus waveguide using a PDMS stamp; (b) Top-view optical micrograph of the transfer printed III-V disk resonator with controlled lateral coupling gap of  $\Delta x = 1 \mu\text{m}$  on top of a Si bus waveguide; (c) Normalised transmission spectra of micro-assembled disk resonator over 1510-1640nm wavelength range containing high extinction multi-mode resonances.

An optical micrograph in Fig. 2(b) shows a hybrid integrated AlGaAs disk resonator evanescently coupled to a Si bus waveguide on the SOI substrate using the aforementioned micro-assembly method, with high loaded Q-factors of  $\approx 2.5 \times 10^4$  and a FSR  $\approx 18\text{nm}$ . The structure has a precisely controlled lateral coupling gap of  $\Delta x = 1 \mu\text{m}$  to promote evanescent coupling to multiple mode families (Fig. 2(c)). The lateral gap can be manipulated during TP to selectively control the mode excitation, an effect previously requiring complex multi-fabrication steps [13].

## 4. FOUR-WAVE MIXING

In addition to the controllable mode coupling, we perform CW four-wave mixing (FWM) experiments using the hybrid all-pass filters micro-assembled by transfer printing. The experimental set-up (Fig. 3(a)) contains two input sources, a high-power pump beam ( $\lambda \approx 1560\text{nm}$ ) and a low-power signal beam ( $\lambda \approx 1585\text{nm}$ ) both TE-polarised. The output light is coupled to an optical spectrum analyser (OSA) for measurement of the FWM spectra containing the pump and signal alongside the output idler peak ( $\lambda \approx 1535\text{nm}$ ), Fig. 3(b). The FWM efficiency is defined as the ratio of the output idler intensity to the input signal intensity. The first demonstrations of FWM from hybrid devices fabricated by a back-end assembly technique are detailed, with efficiencies in the range of  $\sim 25\text{dB}$  from on-chip optical power as low as  $P_p = 2.5\text{mW}$ . The FWM efficiency achieved is comparable to state-of-the-art monolithic silicon devices, with identical Q-factor, at low on-chip optical powers ( $\sim 33\text{dB}$  at  $0.7\text{mW}$ ) [14]. However, AlGaAs devices do not exhibit TPA saturation experienced by silicon when pumped at higher on-chip optical powers, as shown in Fig. 3(b).

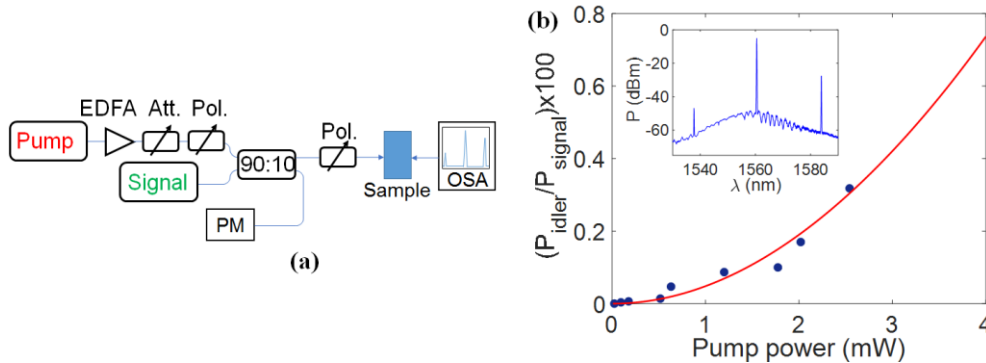


Fig 3. (a) Schematic illustration of measurement setup for FWM experiment. EDFA: Erbium doped fibre amplifier, PM: Power meter, OSA: Optical spectrum analyser; (b) FWM efficiency as a function of on-chip power, showing both experimental data and theoretical curve. (Inset: Measured FWM spectrum captured from OSA showing the idler peak (left), pump peak (centre), and signal peak (right).)

As well as the advantage of increased optical on-chip powers as a method to improve on the FWM efficiency, further optimisation of the hybrid resonator devices through techniques such as dispersion engineering and improved modal confinement can significantly increase the achievable FWM efficiency.

## 5. CONCLUSIONS

We present the heterogeneous integration of III-V micro-disk structures with the SOI platform using a high alignment accuracy transfer printing method. This technique enables the production of high quality hybrid resonator devices with precise control over mode resonance excitation within the disk cavity. Further to this, we present the efficient non-linear conversion of the hybrid devices by the demonstration of FWM at low optical on-chip powers.

## ACKNOWLEDGEMENTS

This work was supported by the EPSRC through *Cornerstone* (EP/L021129/1) and *Parallel Heterogeneous Integration of III-V Devices on Silicon Photonic Chips* (EP/P013570/1). The authors acknowledge the staff of the James Watt Nanofabrication Centre at the University of Glasgow.

## REFERENCES

- [1] J. Doylend and A. Knights: *Laser & Photonics Rev.*, vol. 6, pp. 504–525, 2012.
- [2] M. J. R. Heck, et al: *IEEE J. Sel. Top. Quantum Electron.*, vol. 19, pp. 6100117–6100117, 2013.
- [3] R. Soref: *IEEE J. Sel. Top. Quantum Electron.*, vol. 12, pp. 1678–1687, 2006.
- [4] M. Pu, L. Ottaviano, E. Semenova, and K. Yvind, *Optica.*, vol. 3, pp. 811, 2016.
- [5] J. Leuthold, C. Koos, W. Freude: *Nature photonics*, vol. 4, pp. 535–544, 2010.
- [6] G. I. Stegeman, et al: *Journal of Nonlinear Optical Physics & Materials*, vol. 3, pp. 347–372, 1994.
- [7] M. Pu, et al: *Laser & Photonic Reviews*, vol. 12, pp. 1800111, 2018.
- [8] B. Corbett et al: *Prog. Quantum Electron*, vol. 52, pp. 1–17, 2017.
- [9] J. Zhang et al: *Optics Express*, vol. 26, pp. 8821, 2018.
- [10] C. Bower et al: *Photonics Research*, vol. 5, pp. 23–29, 2017.
- [11] J. McPhillimy et al: *Optics Express*, vol. 26, pp. 297–300, 2018.
- [12] B. Guilhaert et al: *Optics Letters*, vol. 43, pp. 4883–4886, 2018.
- [13] M. Ghulinyan, et al: *IEEE Photonics Technology Letters*, vol. 23, pp. 1166–1168, 2011.
- [14] M. Strain et al: *Optics Letters*, vol. 40, pp. 1274, 2015